

H₂O₂ Electrochemical Sensor Based on *Scutellaria Barbata* Extract Biosynthesized of Gold Nanoparticles

Yaohua Dong^{1*} and Hao Hu¹

¹ College of Marine Science and Engineering, Shanghai Maritime University, No.1550 Haigang Ave, Shanghai, 201306, P.R. China

*E-mail: yhdong@shmtu.edu.cn

Received: 14 September 2016 / Accepted: 18 October 2016 / Published: 10 November 2016

Nobel metal nanoparticles are receiving increasing attention in many fields such as material chemistry, environmental science and pharmaceutical science. In this study, a facial synthesis of a gold nanoparticles (Au NPs) was carried out from *Scutellaria barbata* extract. The synthesized Au NPs was characterized by using UV-vis spectroscopy and X-ray photoelectron spectroscopy. The preparation process was highly rapid since the formation of Au nanoparticles was totally complete within 3 h. We further investigated the electrochemical properties of the biosynthesized Au NPs. A nonenzymatic H₂O₂ electrochemical sensor was shown to be successfully fabricated by using biosynthesized Au NPs. Moreover, the fabricated electrochemical sensor also showed good selectivity.

Keywords: Biosynthesis; *Scutellaria barbata*; Electrocatalysis; Electrochemical sensor; Hydrogen peroxide; Au NPs

1. INTRODUCTION

Currently biologically assisted synthesis plays a vital role in the fabrication of nanomaterials. The use of environmentally benign materials such as plant extract, fungi and bacteria for generating metal or metal oxide NPs is considered as an eco-friendly approach. For example, Jayaseelan et al. [1] reported the synthesis of ZnO NPs using reproducible bacteria (*Aeromonas hydrophila*), as an eco-friendly reducing and capping agent. Roy et al. demonstrated the synthesis of silver nanoparticles using the extracellular filtrate of the fungal strain, *Aspergillus foetidus* MTCC8876 [2]. Kannan and co-workers demonstrated the synthesis of yttrium oxide nanoparticles using *Acalypha indica* leaf extract [3]. They also investigated the antibacterial property of biosynthesized Y₂O₃ and showed an increasing rate of antibacterial behavior with pathogens. Moreover, there are many reports on the

synthesis of metal, semiconductor, and nanomaterial using aloe vera plant extracts [4-6]. Among them, synthesis of inorganic nanomaterials using a plant mediated reducing agent has been found to be more favorable, due to the low cost and high yield.

Gold nanoparticles have had a substantial impact across a diverse range of fields due to their outstanding electrical, optical, catalytic and antimicrobial properties. There are numerous methods for synthesis of Au NPs; however, those methods always involve utilization of toxic reagents and expensive instruments along with very tedious process control. Thus, the facile synthesis of silver nanoparticles with efficient catalytic activity has significant industrial importance. Many previous researchers have highlighted the facile synthesis of Au NPs. For example, Korbekandi and co-worker recently proposed a method for biosynthesis of Au NPs using *Quercus brantii* (oak) leaves hydroalcoholic extract [7]. Hassan and co-workers have also synthesized Au NPs using *Althaea officinalis* radix hydroalcoholic extract [8]. Meng and co-workers demonstrated a biosynthesis of Au NPs using oriental medicinal herb *Gynostemma pentaphyllum* Makino extract [9].

To determine hydrogen peroxide (H_2O_2) in various fields such as pharmaceuticals, biology and food accurately and sensitively is of great importance and has attracted worldwide attention [10]. Varieties of analytical techniques including electrochemiluminescence [11], fluorescence [12] and spectrophotometry [13] have been applied for the determination of H_2O_2 . Nevertheless, certain disadvantages such as high-cost, time-consuming and the requirement of precision instruments and skilled operators have restricted the wide usage of the above-mentioned analytical techniques. Electrochemical technique has been considered as an alternative owing to its simplicity, accuracy, sensitivity, selectivity and low-cost [14-18]. Owing to the fact that H_2O_2 is a by-product of the reactions catalyzed by a great many of oxidase [19], the electro-oxidation of H_2O_2 in electrochemical sensors counts a great deal. When bare electrodes were employed, the irreversible electrochemical oxidation of H_2O_2 occurred with high over-potential [20-24]. What's more, other biological molecules (e.g., ascorbic acid and uric acid) also undergo oxidation within the potential window as H_2O_2 [25, 26]. As a result, the modification of the surface of the electrode has demonstrated to be an effective method to settle the matters. Au NPs is an ideal electrode surface modifier for H_2O_2 electrochemical determination

In our study, *Scutellariae barbata*, extracted from a traditional Chinese plant, has been employed as the reducing agent in the biosynthesis of Au NPs. A series techniques was applied to determine the morphology of the as-synthesized Au NPs. What's more, the biosynthesized Au NPs have demonstrated excellent electrochemical performance towards the determination of hydrogen peroxide.

2. EXPERIMENTS

2.1. Materials

All chemicals are of analytical grade and purchased from Sigma-Aldrich. Dry *Scutellariae barbata* was supplied by local Chinese traditional drug store. Mill-Q water was adopted in the entire experiments. Before the usage, *Scutellariae barbata* was firstly washed by Mill-Q water until the

complete removal of extraneous impurity, subsequently, the wet sample was shade-dried for three days and then dried completely at 70 °C, finally grounded into fine powder.

2.2. Biosynthesis of Au nanoparticles using *Scutellariae barbata*

The *Scutellariae barbata* extract was obtained as follows: *Scutellariae barbata* powder (10 g) was added into water (100 mL), firstly treated with sonication for 15 min and then heated at 70 °C for another 15 min, and finally the mixture was filtrated by filter paper with pore size of 200 nm. To prepare the Au NPs, 20 mL of *Scutellariae barbata* extract was added to 20 mL of H₂AuCl₄ solution and the mixture was sonicated for 1 h. During the formation process of Au NPs, the color of solution will change from pale yellow to purple. After the reaction was complete, the mixture was centrifuged at 10,000 rpm for 30 min and washed by Mill-Q water. The obtained Au NPs were dried in oven at 70°C.

2.3. Characterization

The structure of the biosynthesized Au NPs was characterized by XRD (PW3040/60 X'pert PRO) and the pattern was collected from 10° to 80° in 2θ. The morphology images were measured on Scanning electron microscope (SEM, ZEISS X-MAX). Energy-dispersive X-ray spectroscopy (EDS) was employed for the determination of elemental information. The reduction of Au salt was investigated by the UV-vis spectrophotometer (Shimadzu UV-1601PC) within the range of 300-800 nm. The formation of Au NPs was further confirmed by X-ray photoelectron spectroscopy (XPS, VGESCALAB MKII)

2.4. Electrochemical determination of hydrogen peroxide

A three electrode system was used for electrochemical determination. Au NPs modified glassy carbon electrode (GCE) was used as working electrode, Pt was used as counter electrode and saturated Ag/AgCl was used as reference electrode. The modification of GCE surface was carried out as follows: 5 μL of Au NPs solution (1 mg/mL) was dropped onto the surface of GCE and then dried at room temperature. The electron transfer performance on the original and modified GCE electrodes was evaluated by electrochemical impedance spectroscopy (EIS). The specific experimental settings are as follows: 5 mM [Fe(CN)₆]^{3-/4-} as probe, 0.1 M KCl as supporting electrolyte, 10¹-10⁵ Hz as frequency range and 5 mV as amplitude. As to the determination of hydrogen peroxide using CV method, 0.1M PBS with pH of 7 and the scan range 0-1.0 V with scan rate 50 mV/s were used.

3. RESULTS AND DISCUSSION

The nucleation of Au NPs took place instantaneously after the *Scutellariae barbata* extract was added into H₂AuCl₄ solution, which can be seen from the changeable color of the dispersion from light

yellow to purple. Surface plasmon resonances can be used for confirming the existence of Au NPs since the light at particular wavelength can be absorbed by metallic nanoparticle, and the result demonstrated the formation of Au NPs dispersion. The UV-vis spectrum of biosynthesized Au NPs was also measured. As shown in Fig. 1A, a distinct absorption peak at 465 nm was observed which confirmed the formation of Au NPs, and the result was in consistent with that obtained by surface plasmon resonance. Certain factors (e.g., size, morphology and solvent) will affect the optical property of as-prepared Au NPs. According to the peak position of surface plasmon resonance, the predicated mean size of the formed Au nanoparticles was in the following range 15-30 nm. The interaction of light having wavelength smaller than the particle size of the AuNPs leads to a polarization of free conduction electrons with respect to the heavier ionic core of the AuNPs. Therefore, an electron dipolar oscillation is created and a surface plasmon absorption band is obtained [27, 28].

The TEM image of the biosynthesized Au NPs was shown in Fig. 1B. The Au NPs were in spherical shape with uniform size. The result indicates spherical Au NPs with average size of 26 nm were obtained using biosynthesis method. Besides, dynamic light scattering (DLS) was also employed for measuring the size distribution of Au NPs. As can be seen from Fig. 1C, the mean size calculated from DLS pattern was 24 nm. In addition, the polydispersity index (PDI) calculated was 0.911 for the Au NPs, suggesting the formation of well dispersed colloidal solution. The difference in size as observed from SEM and TEM may be due to the presence of bioactive molecules on Au NPs surface [29].

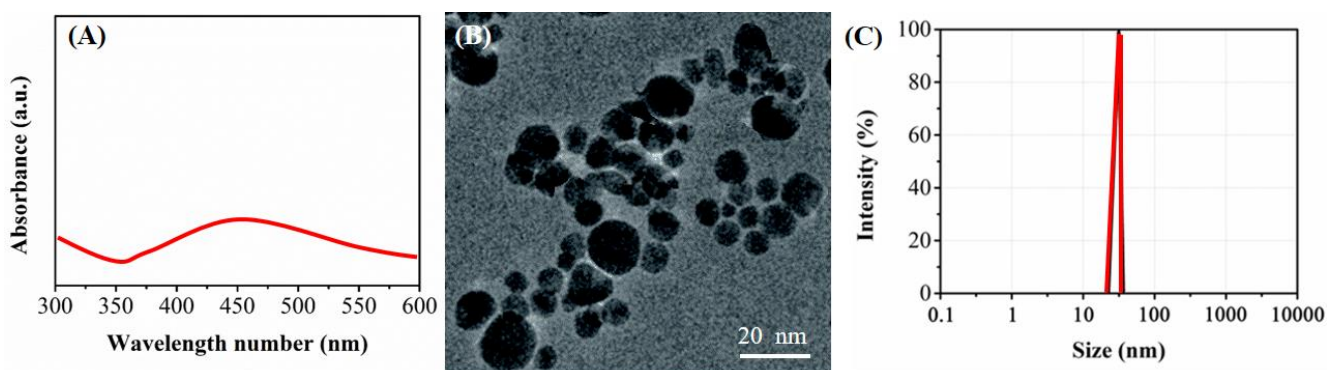


Figure 1. (A) UV-vis spectrum and (B) TEM and (C) DLS pattern of biosynthesized Au NPs.

The formed Au NPs were also characterized by X-ray photoelectron spectroscopy (XPS). As shown in the Au_{4f} high resolution XPS scan (Fig. 2A), the peaks at 88.6 eV and 85.1 eV were ascribed to Au 4f_{5/3} and Au 4f_{5/2}, respectively [30, 31]. Obviously, a shift was observed as compared to the theoretical value of Au⁰ at 88.2 and 84.9 eV, probably resulted from the existence of other biomolecules that composed in the *Scutellariae barbata* extract.

The structure of as-synthesized Au nanoparticles was investigated by XRD. As demonstrated in the XRD spectrum (Fig. 2B), diffraction peaks located at 39.1°, 45.5°, 67.2°, 78.4° and 81.6° were observed, which was corresponding to (111), (200), (220), (311) and (222) planes of fcc

crystallographic structure of Au (JCPDS 4-0783), respectively. The average crystallite size according to Scherrer equation calculated using the width of the (111) peak is found to be 17 nm and is in good agreement with the particle size obtained from the TEM image. In other words, the successful formation of Au NPs was further confirmed.

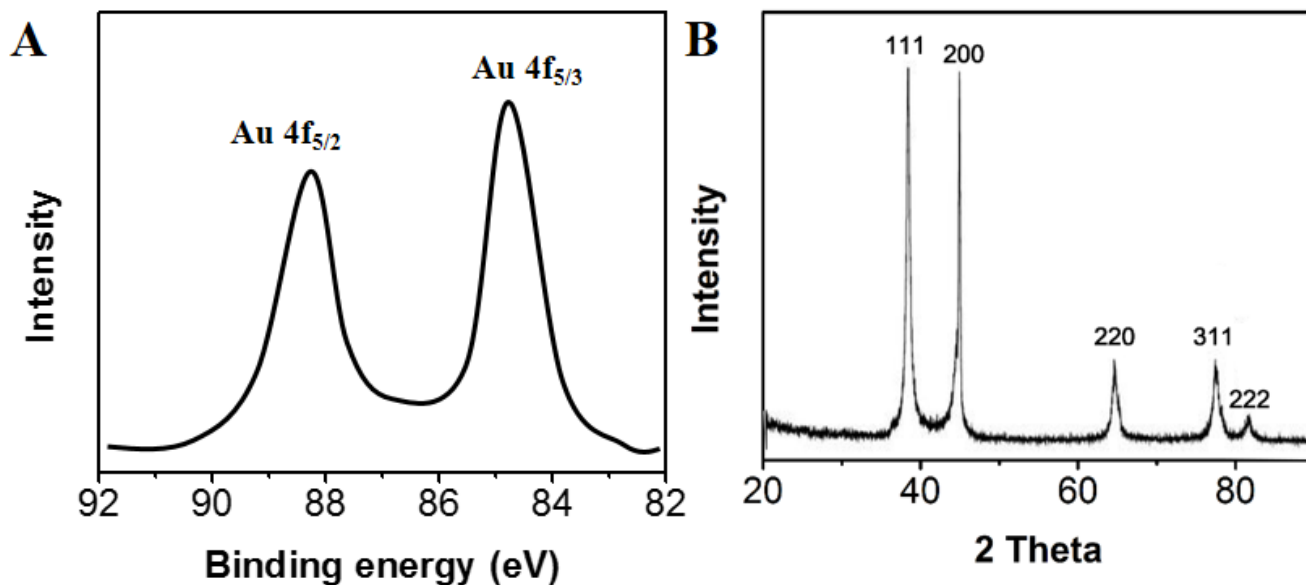


Figure 2. (A) High resolution Au 4f scan and (B) XRD pattern of biosynthesized Au NPs.

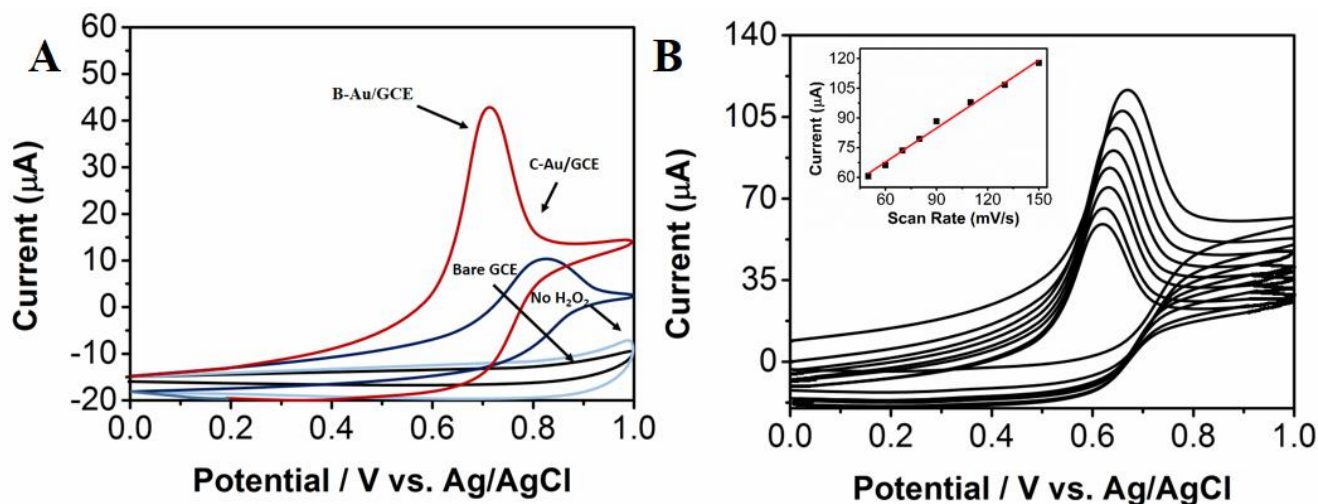


Figure 3. (A) CVs of Bare GCE, C-Au/GCE and B-Au/GCE towards 1 mM H_2O_2 in 0.1 M PBS (pH 7.5). (B) CVs of B-Au/GCE towards 1 mM H_2O_2 in 0.1 M PBS with different scan rate.

To investigate the improvement of biosynthesized Au NPs (B-Au), cyclic voltammograms (CVs) for 1 mM H_2O_2 oxidation were obtained on B-Au/GCE, and the results were compared with that obtained on bare GCE and commercial Au NPs/GCE (C-Au/GCE). As can be seen from the curve obtained on bare GCE (Fig. 3A), no obvious oxidation peak was observed. In contrast, owing to the catalytic activity of Au NPs, a well-defined oxidation peak was observed on C-Au/GCE with the anodic peak potential at 0.81 V. As to the H_2O_2 oxidation on B-Au/GCE, an outstanding

electrocatalytic performance was presented. An oxidation peak at 0.72 V was clearly observed in the process of 1 mM H₂O₂ oxidation on B-Au/GCE, as compared to the smooth CV curve of the B-Au/GCE in PBS. When B-Au/GCE was applied to the H₂O₂ oxidation, the current response was enhanced and the over-potential was lowered, demonstrating the excellent electrocatalytic property of biosynthesized Au NPs that probably resulted from the large surface-to-volume ratio, high electrical conductivity, favorable biocompatible, excellent catalytic ability and surface reaction activity [32, 33].

The effect of scan rates on the oxidation of 1 mM H₂O₂ in PBS with pH of 7.5 at the B-Au/GCE was investigated by CVs. As shown in Fig. 3B, when the scan rate was ranging from 50 to 150 mV/s, the current value of oxidation peak increased gradually with increasing scan rate. The diagram inserted in Fig. 3B showed that the peak currents was related linearly with the scan rates (the regression equation $I_{pa} (\mu A) = 0.5512 v(mV/s) + 32.4517$ with $R^2 = 0.995$). The linear correlation suggested the oxidation of H₂O₂ on B-Au/GCE is controlled by adsorption mechanism [34, 35].

Table 1. Comparison of B-Au/GCE with other Au-based electrodes response to hydrogen peroxide.

Electrode	Detection linear range	Limit of detection	Reference
Mn ₂ O ₃ -Au	10–500 μ M	0.34 μ M	[36]
Au NPs	0.1–160 mM	23 μ M	[37]
Au@poly(m-phenylenediamine)	0.044 to 1.32 mM	4.53 μ M	[38]
B-Au/GCE	1-1000 μ M	0.12 μ M	This work

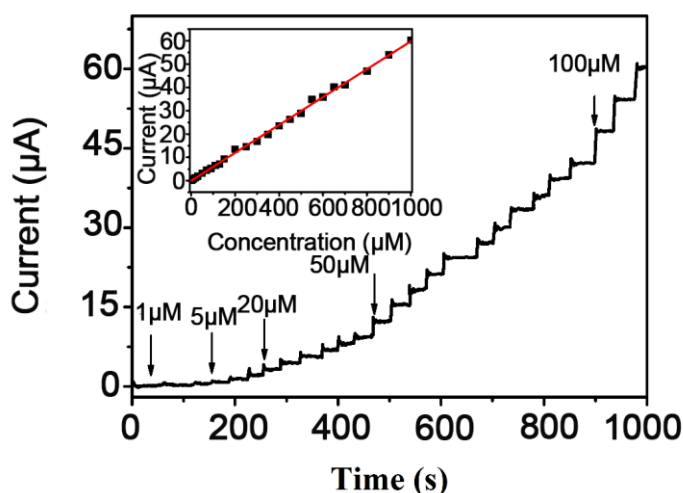


Figure 4. Amperometric response of the B-Au/GCE for the successive addition of H₂O₂. Applied potential: 0.72 V. Inset: The calibration curve for H₂O₂ detection using B-Au/GCE.

For the H₂O₂ oxidation on B-Au/GCE, the response time, linear range and detection limit are of great importance and required to be investigated in detail. Fig. 4 showed the typical amperometric

responses of B-Au/GCE towards the successive addition of H_2O_2 at potential of 0.72 V. At the moment of adding H_2O_2 , the response current increased rapidly and then reached the steady-state within 4 s. Such ultrafast response was resulted from the enhanced electron transfer and electrochemical reaction at the surface of electrode, which could be ascribed to the remarkably conductivity and electrocatalytic property of biosynthesized Au nanoparticles. The amperometric responses of H_2O_2 oxidation on B-Au/GCE was related linearly with the concentrations of H_2O_2 within the concentration range of 1-1000 μM . The regression equation was $I_{\text{pa}} (\mu\text{A}) = 0.0646 c (\mu\text{M}) - 0.029$ with R^2 being 0.998. The calculated detection limit for H_2O_2 was 0.12 μM according to $S/N=3$. For comparison, various H_2O_2 sensors based on Au nanostructure modified electrodes have been listed in Table 1 with respect to the detection limit and linear range.

Chronoamperometry was applied to evaluate anti-interference ability of the B-Au/GCE. As to H_2O_2 sensor, the oxidation of other coexist substances including uric acid (UA) and ascorbic acid (AA) was a significant problem. Fig. 5 showed the amperometric response after the consecutive addition of 0.1 mM H_2O_2 and the mixture of interfering species (AA and UA) with the concentration of 1 mM. It can be seen that a well-defined current response of H_2O_2 was still observed despite the addition of AA and UA, suggesting the excellent anti-interference ability of the B-Au/GCE.

The reproducibility of the proposed sensor towards 0.1 mM H_2O_2 in PBS was investigated by conducting 10 measurements at exactly same conditions. The RSD values calculated was 3.1%, suggesting the excellent repeatable performance. In addition, the storage stability of the B-Au/GCE was also investigated. The current response showed a 2.8% decrease after the B-Au/GCE was stored in fridge for 2 weeks, demonstrating the outstanding stability of the proposed B-Au/GCE sensor for the determination of H_2O_2 .

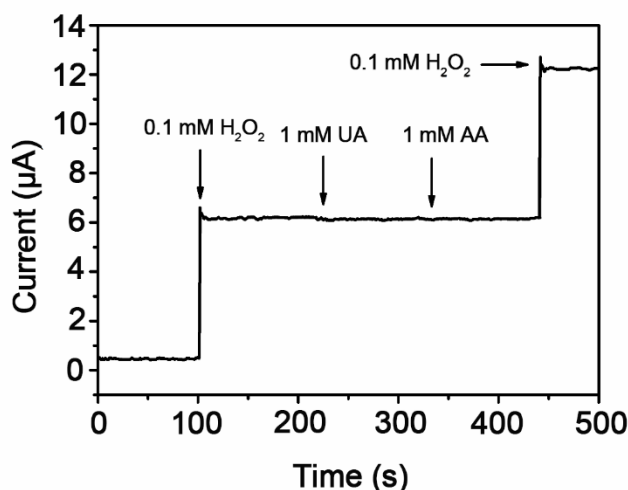


Figure 5. Interfering effect of 1.0 mM AA and 1.0 mM UA on the amperometric response of B-Au/GCE toward 0.1 mM H_2O_2 in pH 7.5 PBS at 0.72 V.

As a real application, B-Au/GCE was used to the determination of H_2O_2 in ultra-high-temperature processed milk. For this aim, 100 μL of the different milk samples was added to 20.0 mL of 0.1 M PBS and the chronoamperometric response of the electrode was recorded at 0.72 V. The

results compared with the value obtained by titration of the sample in acidic media ($2\text{MnO}_4^- + 5\text{H}_2\text{O}_2 + 6\text{H}^+ \rightarrow 2\text{Mn}^{2+} + 5\text{O}_2 + 8\text{H}_2\text{O}$). As shown in Table 2, the good accuracy (recovery) and precision (R.S.D.) demonstrates the reliability of B-Au/GCE for non-enzymatic determination of H_2O_2 in real samples.

Table 2. Determination of H_2O_2 in ultra-high-temperature processed milk with B-Au/GCE ($n = 3$).

Milk sample	B-Au/GCE	Titration	Recovery	RSD
1	16.2	16.1	99.38%	4.21%
2	18.9	18.5	97.88%	2.89%
3	18.5	17.8	96.22%	5.32%

4. CONCLUSIONS

In conclusion, a biosynthesis method with *Scutellariae barbata* as reducing agent was proposed for the preparation of Au NPs. The as-synthesized Au NPs were in spherical shape with average diameter of 24 nm. The GCE modified with biosynthesis Au nanoparticles (B-Au/GCE) demonstrated excellent electrocatalytic performance for the determination of hydrogen peroxide. The linear detection range and detection limit of the proposed sensor were found to be 1-1000 μM and 0.12 μM , respectively.

ACKNOWLEDGEMENTS

This research was supported by the National Natural Science Foundation (51609133)

References

1. C. Jayaseelan, A.A. Rahuman, A.V. Kirthi, S. Marimuthu, T. Santhoshkumar, A. Bagavan, K. Gaurav, L. Karthik and K.V.B. Rao, *Spectrochimica Acta Part A: Molecular and Biomolecular Spectroscopy*, 90 (2012) 78
2. S. Roy, T. Mukherjee, S. Chakraborty and T.K. Das, *Digest Journal of Nanomaterials and Biostructures*, 8 (2013) 197
3. S.K. Kannan and M. Sundrarajan, *Bull Mater Sci*, 38 (2015) 1
4. P.V. Kumar, U. Shameem, P. Kollu, R. Kalyani and S. Pammi, *BioNanoScience*, 5 (2015) 135
5. S. Medda, A. Hajra, U. Dey, P. Bose and N.K. Mondal, *Appl. Nanosci.*, 5 (2015) 875
6. D. Dinesh, K. Murugan, P. Madhiyazhagan, C. Panneerselvam, P.M. Kumar, M. Nicoletti, W. Jiang, G. Benelli, B. Chandramohan and U. Suresh, *Parasitology research*, 114 (2015) 1519
7. H. Korbekandi, M.R. Chitsazi, G. Asghari, R. Bahri Najafi, A. Badii and S. Iravani, *Pharmaceutical biology*, 53 (2015) 807
8. H. Korbekandi, G. Asghari, M.R. Chitsazi, R. Bahri Najafi, A. Badii and S. Iravani, *Artificial cells, nanomedicine, and biotechnology*, (2015) 1
9. F.-B. Meng, L. Wang, H. Xu, C.-C. Liu, P.-C. Hu, W. Lan, J.-X. Song and L.-S. Chen, *Materials Technology: Advanced Performance Materials*, (2015) 1753555715Y.0000000038
10. P.N. Bartlett, P.R. Birkin, J.H. Wang, F. Palmisano and G. De Benedetto, *Anal. Chem.*, 70 (1998) 3685
11. T. Jiao, B.D. Leca-Bouvier, P. Boullanger, L.J. Blum and A.P. Girard-Egrot, *Colloids and Surfaces*

- A: *Physicochemical and Engineering Aspects*, 321 (2008) 143
12. M. Abo, Y. Urano, K. Hanaoka, T. Terai, T. Komatsu and T. Nagano, *Journal of the American Chemical Society*, 133 (2011) 10629
 13. A.C. Pappas, C.D. Stalikas, Y.C. Fiamegos and M.I. Karayannis, *Anal. Chim. Acta.*, 455 (2002) 305
 14. X. Xu, M. Shao, J. Huang, Q. Zhang and L. Ma, *Journal of Nanoscience and Nanotechnology*, 14 (2014) 2635
 15. S.A. Khayyat, S.G. Ansari and A. Umar, *Journal of Nanoscience and Nanotechnology*, 14 (2014) 3569
 16. Y. Zheng, Z. Wang, F. Peng, A. Wang, X. Cai and L. Fu, *Fullerenes, Nanotubes and Carbon Nanostructures*, 24 (2016) 149
 17. F. Han, H. Li, J. Yang, X. Cai and L. Fu, *Physica. E*, 77 (2016) 122
 18. L. Fu, Y. Zheng, Z. Fu, A. Wang and W. Cai, *Bull Mater Sci*, 38 (2015) 611
 19. M. Zhou, Y. Zhai and S. Dong, *Anal. Chem.*, 81 (2009) 5603
 20. F. Xu, Y. Sun, Y. Zhang, Y. Shi, Z. Wen and Z. Li, *Electrochemistry Communications*, 13 (2011) 1131
 21. S. Cinti, F. Arduini, D. Moscone, G. Palleschi and A. Killard, *Sensors*, 14 (2014) 14222
 22. N. Butwong, L. Zhou, W. Ng-eontae, R. Burakham, E. Moore, S. Srijaranai, J.H.T. Luong and J.D. Glennon, *Journal of Electroanalytical Chemistry*, 717–718 (2014) 41
 23. G. Yin, L. Xing, X.-J. Ma and J. Wan, *Chemical Papers*, 68 (2014) 435
 24. Y. Li, H. Wang, H. Zhang, P. Liu, Y. Wang, W. Fang, H. Yang, Y. Li and H. Zhao, *Chemical Communications*, 50 (2014) 5569
 25. H. Lu, S. Yu, Y. Fan, C. Yang and D. Xu, *Colloids and Surfaces B: Biointerfaces*, 101 (2013) 106
 26. Y.-E. Miao, S. He, Y. Zhong, Z. Yang, W.W. Tjiu and T. Liu, *Electrochimica Acta*, 99 (2013) 117
 27. M.M.H. Khalil, E.H. Ismail and F. El-Magdoub, *Arabian Journal of Chemistry*, 5 (2012) 431
 28. K.J. Rao and S. Paria, *ACS Sustainable Chemistry & Engineering*, 3 (2015) 483
 29. S.R. Bhuvanaree, D. Harini, A. Rajaram and R. Rajaram, *Spectrochimica Acta Part A: Molecular and Biomolecular Spectroscopy*, 106 (2013) 190
 30. R. Leppelt, B. Schumacher, V. Plzak, M. Kinne and R. Behm, *J. Catal.*, 244 (2006) 137
 31. J. Li, C.-y. Liu and Y. Liu, *Journal of Materials Chemistry*, 22 (2012) 8426
 32. S. Chen, R. Yuan, Y. Chai and F. Hu, *Microchim. Acta.*, 180 (2013) 15
 33. K. Tang, X. Wu, G. Wang, L. Li, S. Wu, X. Dong, Z. Liu and B. Zhao, *Electrochemistry Communications*, 68 (2016) 90
 34. Q. Guo and M. Li, *Int. J. Electrochem. Sci.*, 11 (2016) 7705
 35. D.K. Yadav, R. Gupta, V. Ganesan, P.K. Sonkar and P.K. Rastogi, *Journal of Applied Electrochemistry*, 46 (2016) 103
 36. B. Saha, S.K. Jana, S. Majumder, B. Satpati and S. Banerjee, *Electrochimica Acta*, 174 (2015) 853
 37. W. Wenchao, J. Ye, Z. Yong, W. Ziying and Z. Tong, *Journal of Semiconductors*, 37 (2016) 013003
 38. F.-B. Meng, H. Xu, W. Li, Q.-W. Liu, S.-M. Gao, X.-C. Ji, Q. Xu and Y. Kong, *Mater. Technol.*, 31 (2016) 255